EMX2 transcriptionally regulates *Nfib* expression in neural progenitor cells during early cortical development.

Running title: EMX2 regulates *Nfib* during cortical development

Jonathan W. C. Lim[1,*], Jens Bunt[1,*,^,†], Caitlin R. Bridges[1], Ching Moey[1], Matisse T. Jacobs[1], Kok-Siong Chen[1], Linda J. Richards[1,2,#,†]

[1] The University of Queensland, Queensland Brain Institute, Brisbane, Queensland, Australia.

[2] The University of Queensland, School of Biomedical Sciences, Brisbane, Queensland, Australia.

Current addresses: ^Princess Maxima Center for Pediatric Oncology, Utrecht, the Netherlands and [#]Department of Neuroscience, Washington University in St Louis Medical School, St Louis MO, USA.

*Authors contributed equally

[†]Authors for correspondence:

Dr Jens Bunt

Email: j.bunt-7@prinsesmaximacentrum.nl

Professor Linda J. Richards

Email: richards@uq.edu.au; linda.richards@wustl.edu

Abstract

The nuclear factor one (NFI) transcription factors play key roles in regulating the onset of both neuronal and glial differentiation during cortical development. Reduced NFI expression results in delayed differentiation, which is associated with neurodevelopmental disorders in humans that include intellectual disability, agenesis of the corpus callosum and macrocephaly. Despite their importance, our understanding of how individual NFI family members are regulated during cortical development remains limited. Here, we demonstrate that in mice, the homeobox transcription factor EMX2 regulates *Nfib* expression in radial glial cells during cortical development. Using a combination of bioinformatics, molecular and histological approaches, we demonstrate that EMX2 is able to bind to the *Nfib* promoter to up-regulate *Nfib* expression. Unexpectedly, *in vivo* over-expression of EMX2 in wildtype animals does not further up-regulate NFIB but instead leads to its down-regulation. Therefore, our findings suggest that EMX2 is capable of both activating and repressing *Nfib*, in a context-dependent manner. This bi-directional control over *Nfib* expression enables fine-tuning of the total level of NFI proteins expressed and could be important for cell-type specific NFI functions.

Keywords

cortical development, EMX2, neuronal differentiation, nuclear factor one, NFIB

Introduction

During development, the timely onset of cellular differentiation is essential to generate the basic anatomic architecture that is required for a fully functional brain. Underpinning this process is the regulation of gene expression, governed by transcription factors that are dynamically expressed in precise spatiotemporal patterns. One such family of transcription factors that are required for the timely differentiation of neural progenitors are the nuclear factor one (NFI) transcription factors. Analyses in mice demonstrate that the expression of these transcription factors in the developing cortex is first detected at approximately embryonic day (E)11.5 (Chaudhry et al. 1997; Plachez et al. 2008), coinciding with the onset of neurogenesis within this region. In humans, haploinsufficiency of the genes *NFIA*, *NFIB* or *NFIX* result in a spectrum of syndromes that are characterised by neurodevelopmental deficits that include macrocephaly, other varying brain malformations and intellectual disability (Zenker et al. 2019).

Nfi knockout mouse models recapitulate the phenotypes reported in humans. These are grossly represented by an expansion of the lateral ventricles and dysgenesis of the corpus callosum, both of which arise due to delayed differentiation of radial glial cells (das Neves et al. 1999; Shu et al. 2003; Barry et al. 2008; Campbell et al. 2008; Piper et al. 2009; Betancourt et al. 2014; Gobius et al. 2016). During embryonic development, the delay in

radial glial cell differentiation in the developing cortex is accompanied by the continued self-renewal of these cells. Consequently, the ventricular zone (VZ) where radial glial cells reside expands and the cortical plate is thinner. Analyses of mouse models at postnatal ages demonstrate enlarged cerebral cortices as compared to wildtype littermates (Campbell et al., 2008; Schanze et al. 2018). This enlargement is presumably due to the subsequent differentiation of the expanded progenitor cell pool that eventually occurs in these mice. As evident by the increased severity of the phenotype when multiple family members are concurrently deleted (Harris et al. 2016; Bunt et al. 2017), tight control of NFI levels is requisite for normal development. Despite their importance, little is known about how the expression of the NFI transcription factors is regulated during brain development.

The transcription factor EMX2 is expressed from approximately E8 in telencephalic progenitors within the dorsal and medial VZ (Simeone et al. 1992; Gulisano et al. 1996; Mallamaci et al. 1998). Analyses of knockout mouse models demonstrate that EMX2 expression during this early period is critical for the specification of the medial cortex. In the absence of EMX2, the hippocampus and cingulate cortex are considerably smaller because of precocious differentiation and depletion of the progenitor cell population (Pellegrini et al. 1996; Yoshida et al. 1997; Shinozaki et al. 2002; Muzio et al. 2005). The neocortical phenotype of *Emx2* knockout mice is considerably milder. Nevertheless, EMX2 plays

78 complex autonomous and non-cell autonomous roles in this region. Among its known roles
79 are regulating the maintenance of the progenitor cell population (Heins et al. 2001;
80 Brancaccio et al. 2010), the differentiation and migration of specific neuronal populations
81 (Mallamaci et al. 2000; Shinozaki et al. 2002), and cortical arealisation (Yoshida et al. 1997;
82 Mallamaci et al. 2000; Bishop et al. 2000; Bishop et al. 2002). Therefore, while EMX2
83 expression is restricted to progenitor cells occupying the VZ, its expression in these cells is
84 critical for regulating many cellular processes throughout cortical development.
85
86 Here, we utilised a bioinformatics approach to identify EMX2 as a candidate transcriptional
87 regulator of *Nfib*. Using a combination of histological and molecular analyses, we further
88 demonstrate that EMX2 is required to drive NFIB expression in radial glial cells during
89 cortical development. Unexpectedly, ectopic over-expression of EMX2 in the developing
90 cortex does not further up-regulate NFIB but instead leads to its down-regulation. Therefore,
91 our findings suggest that EMX2 could function by fine-tuning NFIB expression and is
92 capable of both activating and repressing *Nfib* in this regard.
93

Material and Methods

Animal breeding and tissue collection

All breeding and experiments were performed at the University of Queensland in accordance with the Australian Code of Practice for the Care and Use of Animals for Scientific Purposes and with approval from the University of Queensland Animal Ethics Committee. *Nfib* knockout (*Nfib*^{tm1Rmg}) (Steele-Perkins et al. 2005) and *Emx2* knockout (*Emx2*^{tm1Pgr}) (Pellegrini et al. 1996) mice were maintained on a C57Bl/6 background. To generate timed-pregnant females, male and female mice were placed together overnight and checked the following day for vaginal plugs. This day was designated as E0.5 if a vaginal plug was present. Pregnant dams were euthanised using sodium pentobarbital (Abbott Laboratories) on the day of embryo collection. E13.5 embryos were drop fixed in 4% (w/v) paraformaldehyde (PFA) in phosphate-buffered saline (PBS; pH 7.4) for fluorescence immunohistochemistry or their neocortex dissected in ice-cold sterile PBS and immediately snap frozen for mRNA isolation. E15.5 embryos were transcardially perfused with 0.9% (w/v) saline followed by 4% PFA.

Bioinformatics analyses

Candidate transcriptional regulators of *Nfib* were identified using FIMO software version 5.2.0 (Bailey et al. 2009; Grant et al. 2011). Briefly, the region encompassing the mouse *Nfib* RefSeq transcription start site and 2000 base pairs upstream and downstream of this

(chr4:82503780-82507779 from mm10 assembly) was scanned for putative transcription factor binding sites ($p < 0.0001$) obtained from a database of transcription factor motifs (Jolma et al. 2013). Candidate transcriptional regulators were then filtered to remove transcription factors with low or undetectable expression in the E11.5 forebrain based on expression data from ENCODE mRNA-seq datasets (transcripts per million < 10; dataset identifiers: ENCFF465SNB, ENCFF976OLT) (ENCODE Project Consortium 2012; Davis et al. 2018; He et al. 2020) and the Allen Developing Mouse Brain Atlas (http://developingmouse.brain-map.org) (Thompson et al. 2014). Pairwise alignment of the mouse and human *Nfib* promoter was performed using the EMBOSS Water webtool (Madeira et al. 2019). A subsequent scan for EMX2 binding sites using a less stringent significance threshold ($p < 0.001$) was then performed using FIMO. mRNA expression data of 6 to 16 postconceptional weeks (PCW) human cortical tissue from the BrainSpan Transcriptional Atlas of the Developing Human Brain (http//brainspan.org) (Miller et al. 2014) and GSE25219 (Kang et al. 2011) datasets were analysed and visualised using the R2: Genomics Analysis and Visualization Platform (http://r2.amc.nl) as previously described (Bunt et al. 2010; Bunt et al. 2012). Single-cell mRNA-seq data of SOX2+/PAX6+ cells from 14 to 19 PCW human cortical samples (Thomsen et al. 2016) and E14.5 mouse cortical radial

glial cells (Loo et al. 2019) were tested for statistical significance using Pearson's correlation test in Prism 7 (GraphPad Software).

Immunohistochemistry

Brains of PFA-fixed embryos were removed from the skull and sectioned coronally, sagittally or horizontally at 50 μm on a vibratome. Fluorescence immunohistochemistry was conducted as previously described with minor modifications (Plachez et al. 2008). The primary antibodies that were used are: rabbit anti-NFIB (1:500; HPA003956, Atlas Antibodies), chicken anti-β-galactosidase (1:500; ab9361, Abcam), chicken anti-GFP (1:1000; ab13970, Abcam) and rabbit anti-EMX2 (1:500; HPA065294, Atlas Antibodies). Validation of the specificity of the EMX2 antibody is presented in Supplementary Fig. 1. The specificity of the NFIB antibody was validated previously (Chen et al. 2017). Alexa Fluor 488-conjugated goat anti-chicken (1:500; A-11039, Invitrogen) and Alexa Fluor 555-conjugated goat anti-rabbit (1:500; A-11034, Invitrogen) secondary antibodies were used for detection. Immunofluorescent sections were counterstained with 4',6-diamidino-2-phenylindole, dihydrochloride (DAPI, Invitrogen) to label cell nuclei and coverslipped using ProLong Gold anti-fade reagent (Invitrogen). To reduce technical variability when quantifying

immunofluorescence intensity, matched control sections were mounted on the same slide to ensure identical staining conditions.

Imaging and data analysis

High resolution fluorescence images were acquired using a Diskovery spinning disk confocal system (Spectral Applied Research, Ontaria, Canada) built around a Nikon TiE body equipped with two sCMOS cameras (Andor Zyla 4.2, 2048 x 2048 pixels) and captured with Nikon NIS software (Nikon, Tokyo, Japan). For fluorescence intensity measurements across the different cortical layers, matched neocortical regions of 100 μm width were cropped and analysed using ImageJ software (NIH). To generate fluorescence intensity histograms, cropped sections were divided into 20 bins of equal size across the ventricular to pial surfaces. Fluorescence intensity measurements for *in utero* electroporations were determined by measuring the mean grey value of individual nuclei within the electroporated region. Statistical significance was determined using unpaired t-tests unless otherwise stated, with p-values below 0.05 considered significant. All values are presented as the mean unless otherwise stated, with error bars representing the standard error of the mean. Images in figures are representative images that have been identically cropped, enhanced for contrast and brightness, and pseudo-colored to permit overlay using Adobe Photoshop software.

RNA isolation and quantitative PCR

Total RNA was extracted from E13.5 snap frozen neocortical tissue using TRIzol reagent (Invitrogen) as per the manufacturer's protocol (Life Technologies, USA). RNA was reverse transcribed using SuperScript III First-Strand Synthesis SuperMix (Invitrogen) and Oligo(dT) primers (Invitrogen) as per the manufacturer's instructions. Real-time qPCR was performed with Platinum SYBR Green qPCR SuperMix-UDG (Invitrogen) and 0.25 μM forward and reverse primers on a Rotor-Gene 3000 (Corbett Life Science) as previously described (Bunt et al. 2015). Relative expression was determined using the ΔΔCt method with the housekeeping gene beta-2-microglobulin used as a relative standard. Statistical significance was determined using Welch's t-test. Error bars represent the standard error of the mean. Primers were as previously described (Messina et al. 2010): B2MM 5'-agactgatacatacgcctgcag-3', B2MMC 5'-gcaggttcaaatgaatcttcag-3', mNFI-BE2 5'-gtttttggcatactacgtgcagg-3' and mNFI-BE3C 5'-ctctgatacattgaagactccg-3'.

Plasmid DNA

The mouse *Emx2* coding sequence was amplified from pMXIG-Emx2 (a kind gift from Magdalena Götz) using the following primers containing EcoRI restriction sites: 5'-ATCGGAATCATGTTTCAGCCGGCGCCCAAG-3' and 5'-ATCGGAATTCTTAATCGTCTGAGGTCACATC-3'. The amplified fragment was

subsequently digested and cloned into the EcoRI site within pCAGIG (Addgene plasmid #11159; a kind gift from Connie Cepko) (Matsuda and Cepko 2004) to generate pCAGIG-Emx2. Cloning of the pNfib luciferase plasmid was previously described (Bunt et al. 2015).

Dual-luciferase reporter assays

Human glioblastoma U-251 MG (Ponten and Macintyre 1968) and mouse neuroepithelial NE-4C (Schlett and Madarasz 1997) cell lines were obtained from the American Type Culture Collection (ATCC). Cells were cultured in DMEM (Invitrogen) supplemented with 10% fetal bovine serum at 37°C in a humified atmosphere containing 5% CO_2. Cells were seeded for luciferase reporter assays into a 48-well (U-251) or 96-well (NE-4C) plate 24 hours prior to transfection. Either pCAGIG-Emx2 or pCAGIG were cotransfected with pNfib or the control pGL4.23 luciferase reporter plasmid (Promega) using FuGENE HD (Promega). A control *Renilla* luciferase plasmid (pRL-SV40; Promega) was co-transfected with all transfections as an internal control for normalization of firefly luciferase activity. Luciferase activity was assayed 48 hours after transfection using the Dual-Luciferase Reporter Assay System (Promega). All experimental conditions were tested as three or four independent experiments consisting of technical triplicates. Statistical significance was determined for each cell line using ratio paired t-tests.

203

204 *ChIP-qPCR*

205 NE-4C cells were cultured in DMEM (Invitrogen) supplemented with 10% fetal bovine

206 serum at 37°C in a humified atmosphere containing 5% CO_2. 100 mm cell culture dishes

207 were seeded with cells 24 hours prior to transfection and transfected the following day with

208 the pCAGIG-Emx2 plasmid using FuGENE 6 transfection reagent (Promega) as per the

209 manufacturer's recommendations. Cells were fixed 24 hours after transfection using 1%

210 (w/v) PFA in PBS for 5 minutes. Excess PFA was then quenched with 125 mm glycine.

211 Fixed cells were lysed in lysis buffer (10 mM Tris-HCl pH 8.1, 10 mM NaCl, 3 mM $MgCl_2$,

212 0.5% (v/v) Nonidet P40 substitute solution) supplemented with cOmplete protease inhibitor

213 cocktail (Roche) at 4°C for 20 minutes in order to isolate fixed nuclei. Isolated nuclei were

214 sonicated in sonication buffer (0.1% (w/v) SDS, 1 mM EDTA pH 8.0, 10 mM Tris-HCl pH

215 8.1) supplemented with cOmplete protease inhibitor cocktail (Roche) using the M220

216 focused-ultrasonicator (Covaris) to generate 200 to 500 base pairs chromatin fragments.

217 Chromatin immunoprecipitation (ChIP) was performed by combining chromatin fragments

218 isolated from 2.5 × 10^6 cells and suspended in ChIP buffer (0.087% (w/v) SDS, 0.87 mM

219 EDTA pH 8.0, 8.7 mM Tris-HCl pH 8.1, 150 mM NaCl, 1% (v/v) Triton X-100)

220 supplemented with cOmplete protease inhibitor cocktail (Roche) with 5 µg primary antibody

221 and 50 uL Pierce Protein G magnetic beads (Thermo Scientific). The primary antibodies used

were rabbit anti-EMX2 (HPA065294, Atlas Antibodies) and normal rabbit IgG (#2729, Cell Signaling Technology). Following ChIP, chromatin-bound beads were washed twice with low salt wash buffer (0.1% (w/v) SDS, 1% (v/v) Triton X-100, 2mM EDTA pH 8.0, 150 mM NaCl, 20 mM Tris-HCl pH 8.1), high salt wash buffer (0.1% (w/v) SDS, 1% (v/v) Triton X-100, 2mM EDTA pH 8.0, 500 mM NaCl, 20 mM Tris-HCl pH 8.1), LiCl wash buffer (1% (w/v) sodium deoxycholate, 0.1% (v/v) Nonidet P40 substitute solution, 2 mM EDTA pH 8.0, 250 mM LiCl, 10 mM Tris-HCl pH 8.1) and TE buffer (10 mM Tris-HCl pH 8.1, 1 mM EDTA pH 8.0). Chromatin was eluted from beads using 0.1 M sodium bicarbonate and 1% (w/v) SDS at 65°C for 20 minutes. Eluted chromatin was de-crosslinked at 65°C for 20 hours and sequentially treated with 0.2 mg/mL RNase A (37°C for 1 hour) and 0.4 mg/mL Proteinase K (55°C for 1 hour) before being purified using the QIAquick PCR purification kit (QIAGEN). qPCR was performed on the Rotor-Gene 3000 (Corbett Life Science) using the PowerUp SYBR Green Master Mix (Life Technologies) and the following thermocycler conditions: 2 minutes at 50°C and 2 minutes at 95°C, followed by 40 cycles with 15 seconds denaturation at 95°C and 1 minute annealing and extension at 60°C. Relative enrichment is presented at percent input and statistical significance was determine using unpaired t-tests. Primers used for ChIP-qPCR were: site 1 forward 5'-gagaggctggtgcaaaagg-3', site 1 reverse 5'-ttgaaagattcaccggttcc-3', site 2 forward 5'-tttaaccccgtcctgtcctc-3', site 2 reverse 5'-aggctcttggtttacagggg-3', downstream control forward 5'-actttaggcaccccaaaacg-3',

241 downstream control reverse 5'-gggagcgtctgtagatggac-3', upstream control forward 5'-
242 acccagagagcccaagattc-3' and upstream control reverse 5'-catagccaccatcagcactg-3'. Statistical
243 significance was determined using unpaired t-tests.
244
245 In utero *electroporation*
246 *In utero* electroporation was performed as previously described (Lim et al. 2015). Briefly,
247 pregnant wildtype mice on a CD1 background were anaesthetised with 80-100 mg/kg (body
248 weight) ketamine and 5-10 mg/kg xylazine. An abdominal incision was made to expose the
249 uterus, and 0.5-1.0 µl plasmid DNA (pCAGIG or pCAGIG-Emx2) diluted in sterile PBS was
250 injected through the uterine wall into the medial region of the lateral ventricle of the brain
251 with a pulled glass pipette attached to a Picospritzer III (Parker Hannifin). Electrical pulses
252 (five 35 V pulses of 50 ms applied at 1 second intervals) were then delivered to embryos by
253 electrodes connected to a square-wave ECM 830 electroporator (BTX Harvard Apparatus).
254 Embryos were returned into the abdominal cavity and the abdominal cavity was sutured.
255 Isotonic Ringer's solution was administered subcutaneously and dams were placed in a
256 heated recovery chamber until alert. Buprenorphine (0.05-0.15 mg/kg) was administered
257 orally as an analgesic through ingestion of a flavoured jelly injected with buprenorphine.
258
259
260

Results

EMX2 is a candidate transcriptional regulator of Nfib *expression*

Nfib expression in the developing cortex is first observed at approximately E11.5 (Chaudhry et al. 1997; Plachez et al. 2008) when the cortex is composed primarily of radial glial cells and neurogenesis is just beginning. To identify transcriptional regulators of *Nfib* expression, we undertook a bioinformatics approach by identifying transcription factor motifs present within the *Nfib* promoter and subsequently filtering candidate transcription factors based on their expression at E11.5 in ENCODE mRNA-seq data (Thompson et al. 2014) and the Allen Developing Mouse Brain Atlas (He et al. 2020). Using this approach, we identified EMX2 as a potential regulator of *Nfib* expression. Putative EMX2 binding sites were present within the promoter regions of both human and mouse *Nfib* (Fig. 1A). These binding sites occurred within two highly conserved regions that potentially function as transcriptional regulatory elements (grey boxes in Fig. 1A). Besides these, no further EMX2 binding sites were observed within 2000 base pairs upstream or downstream of the *Nfib* transcriptional start site.

EMX2 expression during cortical development is detected as early as E8.5, where it is expressed in neuroepithelial cells and subsequently in radial glial cells in high caudal to low rostral and high medial to low lateral gradients (Simeone et al. 1992; Gulisano et al. 1996; Mallamaci et al. 1998). While NFIB expression is not limited to the VZ during cortical

development, we previously reported that NFIB expression in radial glial cells followed a similar expression pattern (Bunt et al. 2015). These patterns of expression are replicated within *in situ* hybridization data from the Allen Developing Brain Atlas (Fig. 1B-E). In E11.5 wildtype sagittal sections, the highest expression of *Emx2* and *Nfib* mRNA were observed in the hippocampal primordium and the caudal region of the dorsal cortex, with lower expression detected in rostral regions (Fig. 1B, C). This expression pattern was similarly observed at E13.5 in cells occupying the germinal layer but not within the nascent cortical plate (Fig. 1D, E). At this age, the nascent cortical plate strongly expresses *Nfib*, but *Emx2* is absent within this layer. Furthermore, *Nfib* expression within the cortical plate appears more evenly distributed and does not conform to the graded expression pattern observed within the VZ. These findings suggest that EMX2 could be a transcriptional regulator of *Nfib* within the VZ but is not required to sustain *Nfib* expression in differentiated neurons.

Given that potential EMX2 binding sites identified in the mouse *Nfib* promoter are conserved within the human *NFIB* promoter, we extended our analyses using human RNA-seq data to determine whether the relationship between *Emx2* and *Nfib* expression was similarly conserved in humans. To do this, we first analysed the expression of *EMX2* and *NFIB* mRNA in two independent spatio-temporal transcriptome data sets of human foetal brain samples collected between 6 and 16 PCW (approximately equivalent to E10 to E15.5 in mice) (Kang

et al. 2011; Miller et al. 2014). *NFIB* mRNA expression was similarly correlated with *EMX2* expression in both these data sets (Fig. 1F, G). We also extended our analyses to single-cell RNA sequencing (scRNA-seq) data that was generated from neural progenitor cells of the human and mouse cortex. In a dataset consisting of 186 $SOX2^+$, $PAX6^+$ cells isolated from 14 to 19 PCW human cortical tissues (Thomsen et al. 2016), *NFIB* expression was significantly correlated with *EMX2* expression (Pearson's correlation: r= 0.3086, p<0.0001). Similarly, mouse *Nfib* expression is correlated with *Emx2* expression in cortical radial glial cells isolated from the E14.5 mouse cortex (Pearson's correlation: r= 0.3782, p<0.0001; n = 1605 cells classified as radial glial cells post hoc via unsupervised cell clustering) (Loo et al. 2019). Hence, EMX2 could function as a transcriptional activator of *NFIB* expression during early cortical development in both humans and mice.

EMX2 and NFIB proteins are co-expressed within the ventricular zone during cortical development

We further characterised the expression patterns of EMX2 and NFIB protein by immunofluorescence analyses. To do this, we examined co-expression of EMX2 and the β-galactosidase (βGal) reporter protein in E13.5 *Nfib* heterozygous brains sectioned sagittally, horizontally and coronally. The βGal gene acts as a reporter of NFIB expression as it replaces the second exon of the *Nfib* null allele and is driven by the *Nfib* promoter. Therefore, βGal

318 expression recapitulates expression of endogenous NFIB protein (Steele-Perkins et al. 2005;
319 Piper et al. 2009; Betancourt et al. 2014; Bunt et al. 2015). Immunofluorescence analyses
320 demonstrate that EMX2 and βGal were both highly expressed within the developing dorsal
321 telencephalon at E13.5 (Fig. 2). Lower expression of both proteins was detected in other
322 brain regions and in these regions were predominantly confined to the lining of the ventricles
323 (Fig. 2A). Within the dorsal telencephalon, the expression of EMX2 and βGal was identical
324 to that observed for *Emx2* and *Nfib* mRNA via *in situ* hybridization. Both proteins were co-
325 expressed within the cortical VZ in high caudal to low rostral and high medial to low lateral
326 gradients (Fig. 2B-F). Similarly, EMX2 was not expressed within the nascent cortical plate
327 and βGal staining appeared more evenly distributed within this region.
328
329 *Deletion of* Emx2 *reduces NFIB expression during early development*
330 To further examine the relationship between EMX2 and NFIB expression, we next
331 investigated whether NFIB expression in the developing cortex is altered upon *Emx2*
332 deletion. To do this, we first quantified *Nfib* expression in *Emx2* knockout and wildtype
333 neocortical tissue by qPCR. Relative *Nfib* expression in *Emx2* knockout embryos was
334 reduced by half as compared to wildtype littermates at E13.5 (Fig. 3A). We also quantified
335 *Nfib* expression in these mice at E15.5 but observed no significant differences at this age
336 (data not shown). This discrepancy between the ages could potentially be attributed to

differences in the cellular composition of *Emx2* knockout tissue samples collected at different ages (Pellegrini et al. 1996; Shinozaki et al. 2002). Furthermore, while the expression of EMX2 is confined to radial glial cells that reside within the cortical VZ (Gulisano et al. 1996; Mallamaci et al. 1998), NFIB is expressed not only in radial glial cells but also in postmitotic neurons (Plachez et al. 2008; Piper et al. 2009; Betancourt et al. 2014; Bunt et al. 2015). Hence, if EMX2 regulates *Nfib* in a cell autonomous manner, the reduction in *Nfib* expression is likely to be restricted to radial glial cells that co-express both EMX2 and NFIB.

To further test this hypothesis, we fluorescently stained matched sections of E13.5 *Emx2* knockout and wildtype littermates. The overall staining pattern of NFIB is not altered between wildtype and knockout sections, with high expression observed in the VZ and cortical plate, but not within the intermediate zone (Fig. 3B). We quantified NFIB expression within the cingulate cortex and neocortex by measuring fluorescence intensity at these regions. To normalise for variation in cortical thickness, each section was divided into 20 equal-sized bins spanning the ventricular to marginal zones (Fig 3C, D). The mean fluorescence intensity was then determined for each bin and compared between *Emx2* knockout and wildtype sections. Fluorescence intensity was significantly reduced in the VZ of *Emx2* knockout sections, but not within the intermediate zone or cortical plate. This was true for both the cingulate cortex and neocortex, where fluorescence intensity within the VZ

was reduced by as much as 50% as compared to wildtype sections. Therefore, EMX2 is required for NFIB expression in radial glia.

EMX2 transcriptionally regulates the Nfib *promoter*

We previously cloned the *Nfib* promoter region that encompasses the identified EMX2 binding sites into a luciferase reporter plasmid (Fig. 4A) (Bunt et al. 2015). To further investigate how EMX2 regulates *Nfib* expression, we tested whether luciferase activity driven via this promoter is increased in response to EMX2 over-expression. To do this, we co-transfected mouse NE-4C neuroepithelial cells or human U-251 MG glioblastoma cells with the *Nfib* promoter-driven luciferase plasmid (pNfib) and either an EMX2 over-expression or GFP control plasmid. Co-transfection of the pNfib plasmid with EMX2 increased luciferase activity by a minimum of 3-fold and 5.5-fold as compared to co-transfection with GFP in NE-4C and U-251 cells, respectively (Fig. 4B). We similarly assessed whether EMX2 over-expression had any effect on an empty luciferase reporter plasmid but did not observe any changes in luciferase activity under these conditions (control + EMX2 in Fig. 4C). These findings demonstrate that EMX2 over-expression can activate the *Nfib* promoter.

We next over-expressed EMX2 in NE-4C cells to determine whether the direct binding of EMX2 could be detected by ChIP-qPCR. We designed primer pairs to detect potential

375 binding at both these regions (Sites 1 and 2 in Fig. 4A). As a control, we also designed primer
376 pairs for regions located upstream and downstream that were void of potential EMX2 binding
377 sites (downstream control and upstream control in Fig. 4A). We surveyed the enrichment of
378 EMX2 binding at each of these sites following chromatin immunoprecipitation using an
379 antibody specific for EMX2. EMX2 binding was significantly enriched at the upstream
380 binding region within the *Nfib* promoter (Site 2 in Fig. 4A, D) as compared to all other sites
381 surveyed (Fig. 4D). Hence, our findings demonstrate that EMX2 is capable of directly
382 binding to the *Nfib* promoter to transcriptionally regulate its expression.
383
384 *EMX2 over-expression in the developing cortex down-regulates NFIB expression*
385 As further proof-of-principle, we sought to determine the effect of ectopic EMX2 over-
386 expression on NFIB expression in neural progenitor cells *in vivo*. To do this, we
387 electroporated wildtype embryos at E14.5, an age at which endogenous EMX2 expression is
388 decreasing, and collected embryos for analyses after 24 hours. We electroporated these
389 embryos with a plasmid that encoded for the expression of both *Emx2* and GFP, or a control
390 plasmid encoding GFP only. Coronal sections from both conditions were then stained with
391 antibodies against NFIB and GFP. We compared NFIB expression between electroporated
392 cells within the VZ of both conditions, normalised to adjacent GFP-negative cells within the
393 same sections (Fig. 4E-G). Unexpectedly, over-expression of EMX2 resulted in a reduction

394 in NFIB expression within the VZ where both transcription factors are co-expressed (Fig. 4G,

395 H). Therefore, this finding suggests that besides its role in activating *Nfib* expression, EMX2

396 may also be capable of repressing *Nfib* in a manner dependent on its cellular context.

397

Discussion

In this study, we present evidence demonstrating that EMX2 transcriptionally regulates *Nfib* during early cortical development. Using a computational approach, we identified EMX2 as a candidate transcriptional regulator of *Nfib* with conserved binding sites in human and mouse (Fig. 1A-E). This inference is supported by the positive correlation between their expression levels in published RNA-seq and scRNA-seq datasets (Fig. 1F, G). In line with their known expression patterns, immunofluorescence analyses demonstrate that both proteins are co-expressed within the VZ in similar gradients across the developing cortex (Fig. 2). Furthermore, *Emx2* deletion results in a reduction of NFIB expression within the VZ where both proteins are co-expressed but not the nascent cortical plate (Fig. 3). *In vitro* assays in NE-4C and U-251 MG cells suggest that the regulation of *Nfib* occurs through direct binding of EMX2 at the proximal promoter (Fig. 4A-D). Interestingly, ectopic over-expression of EMX2 via *in utero* electroporation does not up-regulate NFIB but leads to its repression in cells occupying the proliferative zone (Fig. 4E-H). Therefore, our findings suggest that EMX2 may function to fine-tune NFIB expression during cortical development and in this manner contribute to the timely onset of neurogenesis within this system.

We previously described a cohort of 18 individuals with *NFIB* haploinsufficiency (Schanze et al. 2018). While these individuals demonstrated variable phenotypes, the most common

417 neurodevelopmental phenotypes observed were mild intellectual disability and macrocephaly.
418 Analyses of *Nfib* knockout mouse models suggest that deficiencies in neuronal and glial
419 differentiation underlie these defects (Barry et al. 2008; Piper et al. 2009; Betancourt et al.
420 2014; Gobius et al. 2016; Bunt et al. 2017). During cortical development, neuronal
421 differentiation requires neural progenitor cells to switch their mode of cell division from
422 symmetric self-renewing divisions to asymmetric neurogenic divisions. Defects in this switch
423 could result in an expanded progenitor cell population, particularly if progenitor cells
424 continue dividing symmetrically unhindered. Our analyses of *Nfia*; *Nfib* double homozygous
425 knockout embryos demonstrate that the delay in neuronal differentiation observed upon loss
426 of *Nfib* is indeed accompanied by the expansion of the neural progenitor cell pool within the
427 proliferative VZ (Bunt et al. 2017). Transcriptome analyses performed on *Nfib* knockout
428 embryos have also identified mis-regulated genes that may contribute to this phenotype
429 (Betancourt et al. 2014; Bunt et al. 2017). However, our understanding of the underlying
430 molecular pathways encompassing NFIB remains limited. Uncovering these pathways could
431 identify additional genes involved in this process and provide novel insights into congenital
432 disorders of cortical development.
433
434 EMX2 was previously reported as a potential rare cause of schizencephaly in humans but
435 whether this is indeed true requires further investigation (Brunelli et al. 1996; Faiella et al.

1997; Tietjen et al. 2007; Merello et al. 2008; Hehr et al. 2010). Analyses of mouse models demonstrate that EMX2 regulates many processes throughout cortical development. Contradicting NFIB function, EMX2 expression during the initial stages of cortical development is crucial for promoting symmetric cell divisions and maintaining the progenitor cell population (Heins et al. 2001; Brancaccio et al. 2010). Loss of EMX2 during this early period results in precocious cell differentiation (Pellegrini et al. 1996; Yoshida et al. 1997; Shinozaki et al. 2002). Consequently, the progenitor cell population is rapidly depleted and less neurons are generated. Defects in neuronal differentiation are also reported to affect neuronal populations that arise from outside the cortex that do not express EMX2 (Mallamaci et al. 2000; Shinozaki et al. 2002), indicative of a non-autonomous role in the regulation of differentiation of these cell populations. Besides this, contrary to its role during early development, EMX2 expression in progenitor cells at later ages is reported to drive asymmetric divisions (Gangemi et al. 2001; Galli et al. 2002; Gangemi et al. 2006). These findings demonstrate that EMX2 functions in complex roles that require careful examination.

EMX2's ability to regulate both symmetric and asymmetric divisions is intriguing. A potential explanation for this is that EMX2's interaction with other transcription factors or epigenetic factors that are present in different spatiotemporal patterns alters its ability to bind to different genomic regions and regulate different target genes. Additionally, EMX2's

interaction with other transcription factors may be altered depending on the expression level of EMX2 itself. In this manner, EMX2 could potentially repress and activate NFIB expression in neural progenitor cells at different stages of development. Another potential scenario to consider is that the direct binding of EMX2 to the *Nfib* promoter elicits one response (either activation or repression of the promoter), while the opposite effect is brought about through an unknown mechanism that may be independent of EMX2 binding to the *Nfib* locus. Identifying where EMX2 binds in the genome and its target genes will be key to understanding how the function of EMX2 changes throughout development and how it is able to activate and repress NFIB in different contexts. Recent advances in the field of single-cell multiomics will be crucial for this.

To the best of our knowledge, only a few downstream targets of EMX2 have been identified in the central nervous system. These include *Wnt1* (Ligon et al. 2003), *Tenm1* (Beckmann et al. 2011) and *Sox2* (Mariani et al. 2012). Besides these, *Reln* expression is also reduced in *Emx2* knockout mice and is thought to underlie the disorganisation of radial glial fibres observed in these mice (Mallamaci et al. 2000). We previously reported a similar phenotype affecting radial glial cells in the hippocampus of *Nfib* knockout mice (Barry et al. 2008). Together with the present findings, our previous study suggest that reduced NFIB expression could be a contributing factor to the phenotype of radial glial cells in *Emx2* knockout mice.

Besides *Nfib*, the phenotypes of *Nfia* and *Nfix* knockout mice demonstrate that these genes are similarly important for cortical development (das Neves et al. 1999; Shu et al. 2003; Campbell et al. 2008; Gobius et al. 2016). Deletion of multiple *Nfi* genes results in a more severe phenotype as compared to the deletion of single *Nfi* genes, demonstrating that these transcription factors have overlapping but non-redundant functions in regulating these processes (Harris et al. 2016; Bunt et al. 2017). We postulate that the overlapping function of these transcription factors in regulating cell differentiation enables tighter control over the onset of this process during cortical development, as each gene could be individually regulated to fine-tune the total level of NFI expression. In this scenario, the precise expression of each *Nfi* gene will be important for normal development, potentially to ensure that the appropriate proportion of all major cell types are produced. Consequently, understanding how each *Nfi* gene is regulated could reveal important information regarding the regulation of cell differentiation in the developing central nervous system.

In the context of *Nfib*, EMX2 could fine-tune NFIB expression by first repressing its expression earlier in development and then activating *Nfib* expression as neurogenesis begins. This sequence of events explains why EMX2 does not activate *Nfib* prior to E11.5, but both transcription factors are expressed in similar gradients upon NFIB expression. Nevertheless,

493 NFIB could also be repressed prior to E11.5 by other means, such as post-transcriptional
494 regulation or the binding of other transcription factors to the *Nfib* promoter. The 3'
495 untranslated region (3'UTR) of *Nfib* is remarkably long at approximately 6500 nucleotides in
496 length. The microRNA miR-153 (Tsai et al. 2014; Tsuyama et al. 2015) as well as DROSHA
497 (Rolando et al. 2016) are capable of down-regulating *Nfib* mRNA and protein expression
498 through binding at this region. miR-153 is particularly interesting given that its expression in
499 the cortical VZ is detected at E9.5 but its expression in the VZ significantly decreases by
500 E14.5 (Tsuyama et al. 2015). Besides miR-153, the miRNAs miR291-3p, miR183 and miR92
501 are similarly down-regulated by at least 4-fold in rat cortical progenitors when compared
502 between E11 and E13, coinciding with the increase in *Nfib* expression in these cells (Nielsen
503 et al. 2009). Predicted binding sites for each of these miRNAs are present within the *Nfib*
504 3'UTR. Hence, these miRNAs together with miR-153 could play an important role in
505 regulating the onset of *Nfib* expression in neural progenitor cells.
506
507 While other regulators of *Nfib*, such as BRN2 (Fane et al. 2017), ASCL1 (Borromeo et al.
508 2016) and MYC (Mollaoglu et al. 2017) have been reported outside the central nervous
509 system, none of these are likely to play a role in the onset of *Nfib* expression in the central
510 nervous system given their differences in temporal and spatial expression. Nevertheless, since
511 EMX2 expression is limited to radial glial cells throughout corticogenesis, other transcription

512 factors are likely to play key roles in regulating *Nfib* expression, particularly in cell types that
513 do not express EMX2 (Gulisano et al. 1996; Mallamaci et al. 1998) and in the adult brain
514 where NFIB but not EMX2 is widely expressed (Gangemi et al. 2001; Chen et al. 2017).
515 EMX1 is a fitting candidate given its expression in both progenitor cells and postmitotic
516 neurons during cortical development (Gulisano et al. 1996). *In vitro* experiments demonstrate
517 that EMX1 and EMX2 share identical consensus binding motifs (Jolma et al. 2013).
518 Therefore, EMX1 could potentially bind to the EMX2 binding sites that we identified within
519 the *Nfib* promoter to similarly regulate *Nfib* expression in progenitor cells and postmitotic
520 neurons.
521
522 Another scenario that should be considered is the prospect of the NFI transcription factors,
523 including NFIB itself, potentially regulating *Nfib* expression. A super enhancer was recently
524 discovered within the intragenic region adjacent to the *Nfib* locus that is active in neural stem
525 cells. This super enhancer was identified through the enrichment of the Mediator complex
526 within this region, and is also bound by the transcription factor TCF4 in neural stem cells
527 (Moen et al. 2017; Quevedo et al. 2019). Chromatin immunoprecipitation performed with a
528 pan-NFI antibody (recognising all four NFI transcription factors) similarly demonstrates NFI
529 binding at this region (Mateo et al. 2015). Since NFIB is capable of directly interacting with
530 TCF4 as well as MED15 (a subunit of the Mediator complex) (Moen et al. 2017; Quevedo et

al. 2019), the onset of *Nfib* expression followed by its potential binding at this region could result in a feed-forward loop that sustains NFIB expression in the central nervous system. Hence, besides EMX2, NFIB itself could be a potential regulator of *Nfib* expression during cortical development.

In conclusion, this study demonstrates that EMX2 regulates *Nfib* expression in cortical progenitor cells that occupy the dorsal VZ of the developing telencephalon. Given its earlier onset and similar expression patterns when compared to NFIB, EMX2 could be important for driving the initiation of *Nfib* expression during cortical development but may also function to repress *Nfib* expression depending on context. In this way, EMX2 could fine-tune NFIB expression to regulate the onset of cell differentiation during development.

References

Bailey TL, Boden M, Buske FA, Frith M, Grant CE, Clementi L, Ren J, Li WW, Noble WS (2009) MEME SUITE: tools for motif discovery and searching. Nucleic Acids Res 37 (Web Server issue):W202-208. doi:10.1093/nar/gkp335

Barry G, Piper M, Lindwall C, Moldrich R, Mason S, Little E, Sarkar A, Tole S, Gronostajski RM, Richards LJ (2008) Specific glial populations regulate hippocampal morphogenesis. The Journal of neuroscience : the official journal of the Society for Neuroscience 28 (47):12328-12340. doi:10.1523/JNEUROSCI.4000-08.2008

Beckmann J, Vitobello A, Ferralli J, Kenzelmann Broz D, Rijli FM, Chiquet-Ehrismann R (2011) Human teneurin-1 is a direct target of the homeobox transcription factor EMX2 at a novel alternate promoter. BMC Dev Biol 11:35. doi:10.1186/1471-213X-11-35

Betancourt J, Katzman S, Chen B (2014) Nuclear factor one B regulates neural stem cell differentiation and axonal projection of corticofugal neurons. The Journal of comparative neurology 522 (1):30. doi:10.1002/cne.23490

Bishop KM, Goudreau G, O'Leary DD (2000) Regulation of area identity in the mammalian neocortex by Emx2 and Pax6. Science 288 (5464):344-349. doi:10.1126/science.288.5464.344

561 Bishop KM, Rubenstein JLR, O'Leary DDM (2002) Distinct actions of Emx1, Emx2, and
562 Pax6 in regulating the specification of areas in the developing neocortex. Journal of
563 Neuroscience 22 (17):7627-7638
564 Borromeo MD, Savage TK, Kollipara RK, He M, Augustyn A, Osborne JK, Girard L, Minna
565 JD, Gazdar AF, Cobb MH, Johnson JE (2016) ASCL1 and NEUROD1 Reveal
566 Heterogeneity in Pulmonary Neuroendocrine Tumors and Regulate Distinct Genetic
567 Programs. Cell Rep 16 (5):1259-1272. doi:10.1016/j.celrep.2016.06.081
568 Brancaccio M, Pivetta C, Granzotto M, Filippis C, Mallamaci A (2010) Emx2 and Foxg1
569 inhibit gliogenesis and promote neuronogenesis. Stem Cells 28 (7):1206-1218.
570 doi:10.1002/stem.443
571 Brunelli S, Faiella A, Capra V, Nigro V, Simeone A, Cama A, Boncinelli E (1996) Germline
572 mutations in the homeobox gene EMX2 in patients with severe schizencephaly. Nat
573 Genet 12 (1):94-96. doi:10.1038/ng0196-94
574 Bunt J, de Haas TG, Hasselt NE, Zwijnenburg DA, Koster J, Versteeg R, Kool M (2010)
575 Regulation of cell cycle genes and induction of senescence by overexpression of
576 OTX2 in medulloblastoma cell lines. Molecular cancer research : MCR 8 (10):1344-
577 1357. doi:10.1158/1541-7786.MCR-09-0546

578 Bunt J, Hasselt NE, Zwijnenburg DA, Hamdi M, Koster J, Versteeg R, Kool M (2012) OTX2
579 directly activates cell cycle genes and inhibits differentiation in medulloblastoma
580 cells. International journal of cancer 131 (2):E21-32. doi:10.1002/ijc.26474
581 Bunt J, Lim JW, Zhao L, Mason S, Richards LJ (2015) PAX6 does not regulate Nfia and
582 Nfib expression during neocortical development. Scientific Reports 5:10668.
583 doi:10.1038/srep10668
584 Bunt J, Osinski JM, Lim JW, Vidovic D, Ye Y, Zalucki O, O'Connor TR, Harris L,
585 Gronostajski RM, Richards LJ, Piper M (2017) Combined allelic dosage of Nfia and
586 Nfib regulates cortical development. Brain Neurosci Adv 1:2398212817739433.
587 doi:10.1177/2398212817739433
588 Campbell CE, Piper M, Plachez C, Yeh YT, Baizer JS, Osinski JM, Litwack ED, Richards
589 LJ, Gronostajski RM (2008) The transcription factor Nfix is essential for normal brain
590 development. BMC developmental biology 8:52. doi:10.1186/1471-213X-8-52
591 Chaudhry AZ, Lyons GE, Gronostajski RM (1997) Expression patterns of the four nuclear
592 factor I genes during mouse embryogenesis indicate a potential role in development.
593 Developmental dynamics : an official publication of the American Association of
594 Anatomists 208 (3):313-325. doi:10.1002/(SICI)1097-0177(199703)208:3<313::AID-
595 AJA3>3.0.CO;2-L

596 Chen KS, Harris L, Lim JW, Harvey TJ, Piper M, Gronostajski RM, Richards LJ, Bunt J
597 (2017) Differential neuronal and glial expression of nuclear factor I proteins in the
598 cerebral cortex of adult mice. J Comp Neurol. doi:10.1002/cne.24206
599 das Neves L, Duchala CS, Tolentino-Silva F, Haxhiu MA, Colmenares C, Macklin WB,
600 Campbell CE, Butz KG, Gronostajski RM (1999) Disruption of the murine nuclear
601 factor I-A gene (Nfia) results in perinatal lethality, hydrocephalus, and agenesis of the
602 corpus callosum. Proceedings of the National Academy of Sciences of the United
603 States of America 96 (21):11946-11951
604 Davis CA, Hitz BC, Sloan CA, Chan ET, Davidson JM, Gabdank I, Hilton JA, Jain K,
605 Baymuradov UK, Narayanan AK, Onate KC, Graham K, Miyasato SR, Dreszer TR,
606 Strattan JS, Jolanki O, Tanaka FY, Cherry JM (2018) The Encyclopedia of DNA
607 elements (ENCODE): data portal update. Nucleic Acids Res 46 (D1):D794-D801.
608 doi:10.1093/nar/gkx1081
609 ENCODE Project Consortium (2012) An integrated encyclopedia of DNA elements in the
610 human genome. Nature 489 (7414):57-74. doi:10.1038/nature11247
611 Faiella A, Brunelli S, Granata T, D'Incerti L, Cardini R, Lenti C, Battaglia G, Boncinelli E
612 (1997) A number of schizencephaly patients including 2 brothers are heterozygous for
613 germline mutations in the homeobox gene EMX2. Eur J Hum Genet 5 (4):186-190

614 Fane M, Harris L, Smith AG, Piper M (2017) Nuclear factor one transcription factors as
615 epigenetic regulators in cancer. Int J Cancer. doi:10.1002/ijc.30603
616 Galli R, Fiocco R, De Filippis L, Muzio L, Gritti A, Mercurio S, Broccoli V, Pellegrini M,
617 Mallamaci A, Vescovi AL (2002) Emx2 regulates the proliferation of stem cells of
618 the adult mammalian central nervous system. Development 129 (7):1633-1644
619 Gangemi RM, Daga A, Marubbi D, Rosatto N, Capra MC, Corte G (2001) Emx2 in adult
620 neural precursor cells. Mech Dev 109 (2):323-329. doi:10.1016/s0925-
621 4773(01)00546-9
622 Gangemi RM, Daga A, Muzio L, Marubbi D, Cocozza S, Perera M, Verardo S, Bordo D,
623 Griffero F, Capra MC, Mallamaci A, Corte G (2006) Effects of Emx2 inactivation on
624 the gene expression profile of neural precursors. Eur J Neurosci 23 (2):325-334.
625 doi:10.1111/j.1460-9568.2005.04559.x
626 Gobius I, Morcom L, Suarez R, Bunt J, Bukshpun P, Reardon W, Dobyns WB, Rubenstein
627 JL, Barkovich AJ, Sherr EH, Richards LJ (2016) Astroglial-mediated remodeling of
628 the interhemispheric midline is required for the formation of the corpus callosum. Cell
629 Rep 17 (3):735-747. doi:10.1016/j.celrep.2016.09.033
630 Grant CE, Bailey TL, Noble WS (2011) FIMO: scanning for occurrences of a given motif.
631 Bioinformatics 27 (7):1017-1018. doi:10.1093/bioinformatics/btr064

632 Gulisano M, Broccoli V, Pardini C, Boncinelli E (1996) Emx1 and Emx2 show different
633 patterns of expression during proliferation and differentiation of the developing
634 cerebral cortex in the mouse. Eur J Neurosci 8 (5):1037-1050. doi:10.1111/j.1460-
635 9568.1996.tb01590.x
636 Harris L, Zalucki O, Gobius I, McDonald H, Osinki J, Harvey TJ, Essebier A, Vidovic D,
637 Gladwyn-Ng I, Burne TH, Heng JI, Richards LJ, Gronostajski RM, Piper M (2016)
638 Transcriptional regulation of intermediate progenitor cell generation during
639 hippocampal development. Development 143 (24):4620-4630.
640 doi:10.1242/dev.140681
641 He P, Williams BA, Trout D, Marinov GK, Amrhein H, Berghella L, Goh ST, Plajzer-Frick I,
642 Afzal V, Pennacchio LA, Dickel DE, Visel A, Ren B, Hardison RC, Zhang Y, Wold
643 BJ (2020) The changing mouse embryo transcriptome at whole tissue and single-cell
644 resolution. Nature 583 (7818):760-767. doi:10.1038/s41586-020-2536-x
645 Hehr U, Pineda-Alvarez DE, Uyanik G, Hu P, Zhou N, Hehr A, Schell-Apacik C, Altus C,
646 Daumer-Haas C, Meiner A, Steuernagel P, Roessler E, Winkler J, Muenke M (2010)
647 Heterozygous mutations in SIX3 and SHH are associated with schizencephaly and
648 further expand the clinical spectrum of holoprosencephaly. Hum Genet 127 (5):555-
649 561. doi:10.1007/s00439-010-0797-4

650 Heins N, Cremisi F, Malatesta P, Gangemi RM, Corte G, Price J, Goudreau G, Gruss P, Gotz
651 M (2001) Emx2 promotes symmetric cell divisions and a multipotential fate in
652 precursors from the cerebral cortex. Mol Cell Neurosci 18 (5):485-502.
653 doi:10.1006/mcne.2001.1046
654 Holm PC, Mader MT, Haubst N, Wizenmann A, Sigvardsson M, Gotz M (2007) Loss- and
655 gain-of-function analyses reveal targets of Pax6 in the developing mouse
656 telencephalon. Molecular and cellular neurosciences 34 (1):99-119.
657 doi:10.1016/j.mcn.2006.10.008
658 Jolma A, Yan J, Whitington T, Toivonen J, Nitta KR, Rastas P, Morgunova E, Enge M,
659 Taipale M, Wei G, Palin K, Vaquerizas JM, Vincentelli R, Luscombe NM, Hughes
660 TR, Lemaire P, Ukkonen E, Kivioja T, Taipale J (2013) DNA-binding specificities of
661 human transcription factors. Cell 152 (1-2):327-339. doi:10.1016/j.cell.2012.12.009
662 Kang HJ, Kawasawa YI, Cheng F, Zhu Y, Xu X, Li M, Sousa AM, Pletikos M, Meyer KA,
663 Sedmak G, Guennel T, Shin Y, Johnson MB, Krsnik Z, Mayer S, Fertuzinhos S,
664 Umlauf S, Lisgo SN, Vortmeyer A, Weinberger DR, Mane S, Hyde TM, Huttner A,
665 Reimers M, Kleinman JE, Sestan N (2011) Spatio-temporal transcriptome of the
666 human brain. Nature 478 (7370):483-489. doi:10.1038/nature10523
667 Ligon KL, Echelard Y, Assimacopoulos S, Danielian PS, Kaing S, Grove EA, McMahon AP,
668 Rowitch DH (2003) Loss of Emx2 function leads to ectopic expression of Wnt1 in the

669 developing telencephalon and cortical dysplasia. Development 130 (10):2275-2287.
670 doi:10.1242/dev.00421
671 Lim JW, Donahoo AL, Bunt J, Edwards TJ, Fenlon LR, Liu Y, Zhou J, Moldrich RX, Piper
672 M, Gobius I, Bailey TL, Wray NR, Kessaris N, Poo MM, Rubenstein JL, Richards LJ
673 (2015) EMX1 regulates NRP1-mediated wiring of the mouse anterior cingulate
674 cortex. Development 142 (21):3746-3757. doi:10.1242/dev.119909
675 Loo L, Simon JM, Xing L, McCoy ES, Niehaus JK, Guo J, Anton ES, Zylka MJ (2019)
676 Single-cell transcriptomic analysis of mouse neocortical development. Nat Commun
677 10 (1):134. doi:10.1038/s41467-018-08079-9
678 Lopez-Bendito G, Chan CH, Mallamaci A, Parnavelas J, Molnar Z (2002) Role of Emx2 in
679 the development of the reciprocal connectivity between cortex and thalamus. J Comp
680 Neurol 451 (2):153-169. doi:10.1002/cne.10345
681 Madeira F, Park YM, Lee J, Buso N, Gur T, Madhusoodanan N, Basutkar P, Tivey ARN,
682 Potter SC, Finn RD, Lopez R (2019) The EMBL-EBI search and sequence analysis
683 tools APIs in 2019. Nucleic Acids Res 47 (W1):W636-W641.
684 doi:10.1093/nar/gkz268
685 Mallamaci A, Iannone R, Briata P, Pintonello L, Mercurio S, Boncinelli E, Corte G (1998)
686 EMX2 protein in the developing mouse brain and olfactory area. Mech Dev 77
687 (2):165-172

688 Mallamaci A, Muzio L, Chan CH, Parnavelas J, Boncinelli E (2000) Area identity shifts in
689 the early cerebral cortex of Emx2-/- mutant mice. Nat Neurosci 3 (7):679-686.
690 doi:10.1038/76630
691 Mariani J, Favaro R, Lancini C, Vaccari G, Ferri AL, Bertolini J, Tonoli D, Latorre E, Caccia
692 R, Ronchi A, Ottolenghi S, Miyagi S, Okuda A, Zappavigna V, Nicolis SK (2012)
693 Emx2 is a dose-dependent negative regulator of Sox2 telencephalic enhancers.
694 Nucleic Acids Res 40 (14):6461-6476. doi:10.1093/nar/gks295
695 Mateo JL, van den Berg DL, Haeussler M, Drechsel D, Gaber ZB, Castro DS, Robson P, Lu
696 QR, Crawford GE, Flicek P, Ettwiller L, Wittbrodt J, Guillemot F, Martynoga B
697 (2015) Characterization of the neural stem cell gene regulatory network identifies
698 OLIG2 as a multifunctional regulator of self-renewal. Genome Res 25 (1):41-56.
699 doi:10.1101/gr.173435.114
700 Matsuda T, Cepko CL (2004) Electroporation and RNA interference in the rodent retina in
701 vivo and in vitro. Proc Natl Acad Sci U S A 101 (1):16-22.
702 doi:10.1073/pnas.2235688100
703 Merello E, Swanson E, De Marco P, Akhter M, Striano P, Rossi A, Cama A, Leventer RJ,
704 Guerrini R, Capra V, Dobyns WB (2008) No major role for the EMX2 gene in
705 schizencephaly. Am J Med Genet A 146A (9):1142-1150. doi:10.1002/ajmg.a.32264

706 Messina G, Biressi S, Monteverde S, Magli A, Cassano M, Perani L, Roncaglia E, Tagliafico
707 E, Starnes L, Campbell CE, Grossi M, Goldhamer DJ, Gronostajski RM, Cossu G
708 (2010) Nfix regulates fetal-specific transcription in developing skeletal muscle. Cell
709 140 (4):554-566. doi:10.1016/j.cell.2010.01.027
710 Miller JA, Ding SL, Sunkin SM, Smith KA, Ng L, Szafer A, Ebbert A, Riley ZL, Royall JJ,
711 Aiona K, Arnold JM, Bennet C, Bertagnolli D, Brouner K, Butler S, Caldejon S,
712 Carey A, Cuhaciyan C, Dalley RA, Dee N, Dolbeare TA, Facer BA, Feng D, Fliss TP,
713 Gee G, Goldy J, Gourley L, Gregor BW, Gu G, Howard RE, Jochim JM, Kuan CL,
714 Lau C, Lee CK, Lee F, Lemon TA, Lesnar P, McMurray B, Mastan N, Mosqueda N,
715 Naluai-Cecchini T, Ngo NK, Nyhus J, Oldre A, Olson E, Parente J, Parker PD, Parry
716 SE, Stevens A, Pletikos M, Reding M, Roll K, Sandman D, Sarreal M, Shapouri S,
717 Shapovalova NV, Shen EH, Sjoquist N, Slaughterbeck CR, Smith M, Sodt AJ,
718 Williams D, Zollei L, Fischl B, Gerstein MB, Geschwind DH, Glass IA, Hawrylycz
719 MJ, Hevner RF, Huang H, Jones AR, Knowles JA, Levitt P, Phillips JW, Sestan N,
720 Wohnoutka P, Dang C, Bernard A, Hohmann JG, Lein ES (2014) Transcriptional
721 landscape of the prenatal human brain. Nature 508 (7495):199-206.
722 doi:10.1038/nature13185
723 Moen MJ, Adams HH, Brandsma JH, Dekkers DH, Akinci U, Karkampouna S, Quevedo M,
724 Kockx CE, Ozgur Z, van IWF, Demmers J, Poot RA (2017) An interaction network

of mental disorder proteins in neural stem cells. Transl Psychiatry 7 (4):e1082. doi:10.1038/tp.2017.52

Mollaoglu G, Guthrie MR, Bohm S, Bragelmann J, Can I, Ballieu PM, Marx A, George J, Heinen C, Chalishazar MD, Cheng H, Ireland AS, Denning KE, Mukhopadhyay A, Vahrenkamp JM, Berrett KC, Mosbruger TL, Wang J, Kohan JL, Salama ME, Witt BL, Peifer M, Thomas RK, Gertz J, Johnson JE, Gazdar AF, Wechsler-Reya RJ, Sos ML, Oliver TG (2017) MYC Drives Progression of Small Cell Lung Cancer to a Variant Neuroendocrine Subtype with Vulnerability to Aurora Kinase Inhibition. Cancer Cell 31 (2):270-285. doi:10.1016/j.ccell.2016.12.005

Muzio L, Soria JM, Pannese M, Piccolo S, Mallamaci A (2005) A mutually stimulating loop involving emx2 and canonical wnt signalling specifically promotes expansion of occipital cortex and hippocampus. Cereb Cortex 15 (12):2021-2028. doi:10.1093/cercor/bhi077

Nielsen JA, Lau P, Maric D, Barker JL, Hudson LD (2009) Integrating microRNA and mRNA expression profiles of neuronal progenitors to identify regulatory networks underlying the onset of cortical neurogenesis. BMC Neurosci 10:98. doi:10.1186/1471-2202-10-98

Pellegrini M, Mansouri A, Simeone A, Boncinelli E, Gruss P (1996) Dentate gyrus formation requires Emx2. Development 122 (12):3893-3898

744 Piper M, Moldrich RX, Lindwall C, Little E, Barry G, Mason S, Sunn N, Kurniawan ND,
745 Gronostajski RM, Richards LJ (2009) Multiple non-cell-autonomous defects underlie
746 neocortical callosal dysgenesis in Nfib-deficient mice. Neural development 4:43.
747 doi:10.1186/1749-8104-4-43
748 Plachez C, Lindwall C, Sunn N, Piper M, Moldrich RX, Campbell CE, Osinski JM,
749 Gronostajski RM, Richards LJ (2008) Nuclear factor I gene expression in the
750 developing forebrain. The Journal of comparative neurology 508 (3):385-401.
751 doi:10.1002/cne.21645
752 Ponten J, Macintyre EH (1968) Long term culture of normal and neoplastic human glia. Acta
753 pathologica et microbiologica Scandinavica 74 (4):465-486
754 Quevedo M, Meert L, Dekker MR, Dekkers DHW, Brandsma JH, van den Berg DLC, Ozgur
755 Z, van IWFJ, Demmers J, Fornerod M, Poot RA (2019) Mediator complex interaction
756 partners organize the transcriptional network that defines neural stem cells. Nat
757 Commun 10 (1):2669. doi:10.1038/s41467-019-10502-8
758 Rolando C, Erni A, Grison A, Beattie R, Engler A, Gokhale PJ, Milo M, Wegleiter T,
759 Jessberger S, Taylor V (2016) Multipotency of adult hippocampal NSCs in vivo is
760 restricted by Drosha/NFIB. Cell Stem Cell 19 (5):653-662.
761 doi:10.1016/j.stem.2016.07.003

762 Schanze I, Bunt J, Lim JWC, Schanze D, Dean RJ, Alders M, Blanchet P, Attie-Bitach T,
763 Berland S, Boogert S, Boppudi S, Bridges CJ, Cho MT, Dobyns WB, Donnai D,
764 Douglas J, Earl DL, Edwards TJ, Faivre L, Fregeau B, Genevieve D, Gerard M,
765 Gatinois V, Holder-Espinasse M, Huth SF, Izumi K, Kerr B, Lacaze E, Lakeman P,
766 Mahida S, Mirzaa GM, Morgan SM, Nowak C, Peeters H, Petit F, Pilz DT,
767 Puechberty J, Reinstein E, Riviere JB, Santani AB, Schneider A, Sherr EH, Smith-
768 Hicks C, Wieland I, Zackai E, Zhao X, Gronostajski RM, Zenker M, Richards LJ
769 (2018) NFIB Haploinsufficiency Is Associated with Intellectual Disability and
770 Macrocephaly. Am J Hum Genet 103 (5):752-768. doi:10.1016/j.ajhg.2018.10.006

771 Schlett K, Madarasz E (1997) Retinoic acid induced neural differentiation in a
772 neuroectodermal cell line immortalized by p53 deficiency. Journal of neuroscience
773 research 47 (4):405-415

774 Shinozaki K, Miyagi T, Yoshida M, Miyata T, Ogawa M, Aizawa S, Suda Y (2002) Absence
775 of Cajal-Retzius cells and subplate neurons associated with defects of tangential cell
776 migration from ganglionic eminence in Emx1/2 double mutant cerebral cortex.
777 Development 129 (14):3479-3492

778 Shu T, Butz KG, Plachez C, Gronostajski RM, Richards LJ (2003) Abnormal development of
779 forebrain midline glia and commissural projections in Nfia knock-out mice. The
780 Journal of neuroscience 23 (1):203-212

781 Simeone A, Gulisano M, Acampora D, Stornaiuolo A, Rambaldi M, Boncinelli E (1992) Two
782 vertebrate homeobox genes related to the Drosophila empty spiracles gene are
783 expressed in the embryonic cerebral cortex. EMBO J 11 (7):2541-2550
784 Steele-Perkins G, Plachez C, Butz KG, Yang G, Bachurski CJ, Kinsman SL, Litwack ED,
785 Richards LJ, Gronostajski RM (2005) The transcription factor gene Nfib is essential
786 for both lung maturation and brain development. Molecular and cellular biology 25
787 (2):685-698. doi:10.1128/MCB.25.2.685-698.2005
788 Thompson CL, Ng L, Menon V, Martinez S, Lee CK, Glattfelder K, Sunkin SM, Henry A,
789 Lau C, Dang C, Garcia-Lopez R, Martinez-Ferre A, Pombero A, Rubenstein JLR,
790 Wakeman WB, Hohmann J, Dee N, Sodt AJ, Young R, Smith K, Nguyen TN, Kidney
791 J, Kuan L, Jeromin A, Kaykas A, Miller J, Page D, Orta G, Bernard A, Riley Z, Smith
792 S, Wohnoutka P, Hawrylycz MJ, Puelles L, Jones AR (2014) A high-resolution
793 spatiotemporal atlas of gene expression of the developing mouse brain. Neuron 83
794 (2):309-323. doi:10.1016/j.neuron.2014.05.033
795 Thomsen ER, Mich JK, Yao Z, Hodge RD, Doyle AM, Jang S, Shehata SI, Nelson AM,
796 Shapovalova NV, Levi BP, Ramanathan S (2016) Fixed single-cell transcriptomic
797 characterization of human radial glial diversity. Nat Methods 13 (1):87-93.
798 doi:10.1038/nmeth.3629

799 Tietjen I, Bodell A, Apse K, Mendonza AM, Chang BS, Shaw GM, Barkovich AJ, Lammer
800 EJ, Walsh CA (2007) Comprehensive EMX2 genotyping of a large schizencephaly
801 case series. Am J Med Genet A 143A (12):1313-1316. doi:10.1002/ajmg.a.31767
802 Tsai PC, Bake S, Balaraman S, Rawlings J, Holgate RR, Dubois D, Miranda RC (2014) MiR-
803 153 targets the nuclear factor-1 family and protects against teratogenic effects of
804 ethanol exposure in fetal neural stem cells. Biology open 3 (8):741-758.
805 doi:10.1242/bio.20147765
806 Tsuyama J, Bunt J, Richards LJ, Iwanari H, Mochizuki Y, Hamakubo T, Shimazaki T, Okano
807 H (2015) MicroRNA-153 Regulates the Acquisition of Gliogenic Competence by
808 Neural Stem Cells. Stem Cell Reports 5 (3):9. doi:10.1016/j.stemcr.2015.06.006
809 Walther C, Gruss P (1991) Pax-6, a murine paired box gene, is expressed in the developing
810 CNS. Development 113 (4):1435-1449
811 Yoshida M, Suda Y, Matsuo I, Miyamoto N, Takeda N, Kuratani S, Aizawa S (1997) Emx1
812 and Emx2 functions in development of dorsal telencephalon. Development 124
813 (1):101-111
814 Zenker M, Bunt J, Schanze I, Schanze D, Piper M, Priolo M, Gerkes EH, Gronostajski RM,
815 Richards LJ, Vogt J, Wessels MW, Hennekam RC (2019) Variants in nuclear factor I
816 genes influence growth and development. Am J Med Genet C Semin Med Genet 181
817 (4):611-626. doi:10.1002/ajmg.c.31747

818

819

820

821

Acknowledgements

We thank the staff of the University of Queensland Biological Resources (UQBR) animal facility and the QBI Advanced Microimaging and Analysis Facility for their expertise and support in this project. We thank Peter Gruss (Max Planck Society, Munich, Germany) for providing the *Emx2* knockout mouse line and Magdalena Götz for providing the pMXIG-Emx2 plasmid. We are also grateful to Yunan Ye and Elizabeth Vanderkop for their assistance with experiments.

Funding

This work was supported by the National Health and Medical Research Council (GNT1100443 and GNT1120615) and the Australian Research Council (DP150104748 and DP200102363). Students were supported by the University of Queensland (UQ Centennial Scholarship to JWCL and International Postgraduate Student Scholarship to K-SC) and the Australian Government (Research Training Program Scholarship to JWCL).

Author contributions

Conceptualization: JWCL, JB, LJR; Formal analysis and investigation: JWCL, JB, CRB, CM, MTJ, K-SC; Writing - original draft preparation: JWCL, JB, LJR; Writing - review and

840 editing: JWCL, JB, CRB, CM, MTJ, K-SC, LJR; Resources: RMG; Supervision: JWCL, JB,

841 LJR

842

843 **Compliance with Ethical Standards**

844

845 **Conflicts of interest**

846 All authors declare that they have no conflicts of interest.

847

848 **Ethical Approval**

849 All applicable international, national, and/or institutional guidelines for the care and use of

850 animals were followed. This article does not contain any studies with human participants

851 performed by any of the authors.

852

853

Figure Legends

Fig. 1

EMX2 is a candidate transcriptional regulator of NFIB. (*A*) Schematic of the proximal promoter region of *Nfib* in mouse and human. Solid blue bars represent the 5' untranslated region and exon 1 of *Nfib*. Red boxes denote potential EMX2 binding sites as identified using the motif finding tool FIMO (Grant et al. 2011), with the grey boxes demonstrating sequence conservation within these regions (mouse mm10 and human hg38). Scale bar represents 1000 base pairs. (*B-E*) *In situ* hybridization images of E11.5 and E13.5 sagittal sections probed for *Emx2* and *Nfib* expression were obtained from the Allen Developing Mouse Brain Atlas (Thompson et al. 2014), demonstrating similar expression gradients. Scale bar represents 400 μm. Image credit: Allen Developing Mouse Brain Atlas (http://developingmouse.brain-map.org). Image identifiers: image 7 of 18 from experiment 100047257 (E11.5 *Emx2*), image 11 of 16 from experiment 100041799 (E13.5 *Emx2*), image 7 of 16 from experiment 100054279 (E11.5 *Nfib*), and image 14 of 18 from experiment 100054417 (E13.5 *Nfib*). (*F*, *G*) Correlation of *EMX2* (x-axis) and *NFIB* (y-axis) mRNA expression in human fetal brain samples from 6 to 16 postconceptional weeks (PCW) from Brainspan (Miller et al. 2014) and GSE25219 (Kang et al. 2011), respectively. Each colour represents a different PCW.

873 **Fig. 2**

874 Similar expression patterns of EMX2 and NFIB in the developing brain. (*A*) Representative
875 immunofluorescent images of sagittal, horizontal and coronal sections of E13.5 *Nfib*
876 heterozygous brains stained for EMX2 (red) and a β-galactoside (βGal) reporter driven
877 through the *Nfib* locus (green). Scale bar represents 500 μm. (*B*, *C*) High-powered
878 monochrome images of the dorsal telencephalon stained for EMX2 and βGal, respectively.
879 Scale bar represents 100 μm. (*D-F*) High-powered immunofluorescent images of different
880 brain regions represented by insets in (*B*).

881

882 **Fig. 3**

883 *Nfib* mRNA and protein expression is reduced in the E13.5 *Emx2* knockout cortex. (*A*)
884 Relative *Nfib* mRNA levels in the E13.5 neocortex of wildtype (n=4) and *Emx2* knockout
885 (n=3) littermates as determined by qPCR. Statistical significance was determined using
886 Welch's t-test ($p = 0.0007$). (*B*) Representative high-powered immunofluorescent images of
887 the cingulate and neocortices of E13.5 wildtype and *Emx2* knockout coronal sections stained
888 for NFIB (red) and DAPI nuclear stain (blue). Scale bar represents 50 μm. (*C*, *D*) Mean
889 fluorescence intensity of NFIB protein expression in the cingulate cortex (*C*) and neocortex
890 (*D*) of wildtype (blue) and *Emx2* knockout (red) sections. Fluorescence intensity was
891 measured for each section using 20 equally spaced bins that extended from the ventricular to

892 pial surfaces (n = 6-7 per genotype). Statistical significance was determined using unpaired t-
893 tests.
894
895 **Fig. 4**
896 EMX2 regulates the *Nfib* promoter and fine-tunes NFIB expression. (*A*) Schematic of the
897 proximal promoter region of *Nfib* adapted from Fig. 1. Solid blue bars represent the 5'
898 untranslated region and exon 1 of *Nfib*. Red boxes enclosed by grey boxes denote potential
899 EMX2 binding sites within potential regulatory elements shared between human and mouse.
900 The dashed line in magenta depicts the region cloned into the pNfib luciferase plasmid.
901 Primers pairs for ChIP-qPCR are depicted by adjoining black boxes. Scale bar represents
902 1000 base pairs. (*B*) Relative fold change in luciferase activity measured in NE-4C and U-
903 251 MG cells. Each data point represents an individual biological replicate, in which relative
904 luciferase activity of the *Nfib* promoter co-transfected with EMX2 was determined upon
905 normalisation to GFP control. Relative luciferase activity increased significantly upon EMX2
906 over-expression ($p = 0.0466$ (NE-4C) and $p = 0.0068$ (U-251) in ratio paired t-tests). (*C*)
907 Representative luciferase assay performed in NE-4C cells, corresponding to the biological
908 replicate outlined in red in (*B*). Data points represent individual technical replicates
909 normalised to luciferase activity obtained from the respective luciferase plasmids co-
910 transfected with GFP. (*D*) EMX2 binding (represented as % input) as assayed by ChIP-

911 qPCR. Statistical significance was determined using unpaired t-tests. EMX2 binding was
912 statistically significant at site 2 as compared to all other tested regions ($p = 0.0219$, 0.0340
913 and 0.0176 when compared to downstream control, site 1 and upstream control, respectively).
914 Open and closed circles represent individual biological replicates from separate experiments
915 ($n = 2$). (*E*) Representative immunofluorescent images of E15.5 wildtype coronal sections
916 electroporated at E14.5 with control or *Emx2* plasmids. Sections were stained for NFIB
917 (magenta) and GFP (green). Scale bar represents 50 μm. (*F*, *G*) High-powered images
918 represented by insets in (*E*). Yellow arrowheads denote electroporated GFP-positive cells.
919 Cyan arrows denote cells without GFP expression. (*H*) Violin plots representing relative
920 NFIB expression in the VZ normalised to mean expression of adjacent GFP-negative cells
921 within the same sections. Statistical significance was determined using a Mann-Whitney test.
922 Dotted lines within individual plots denote the lower quartile, median and upper quartile
923 ($n = 7$-9 per condition with 5 electroporated and 5 GFP-negative cells analysed per animal).
924

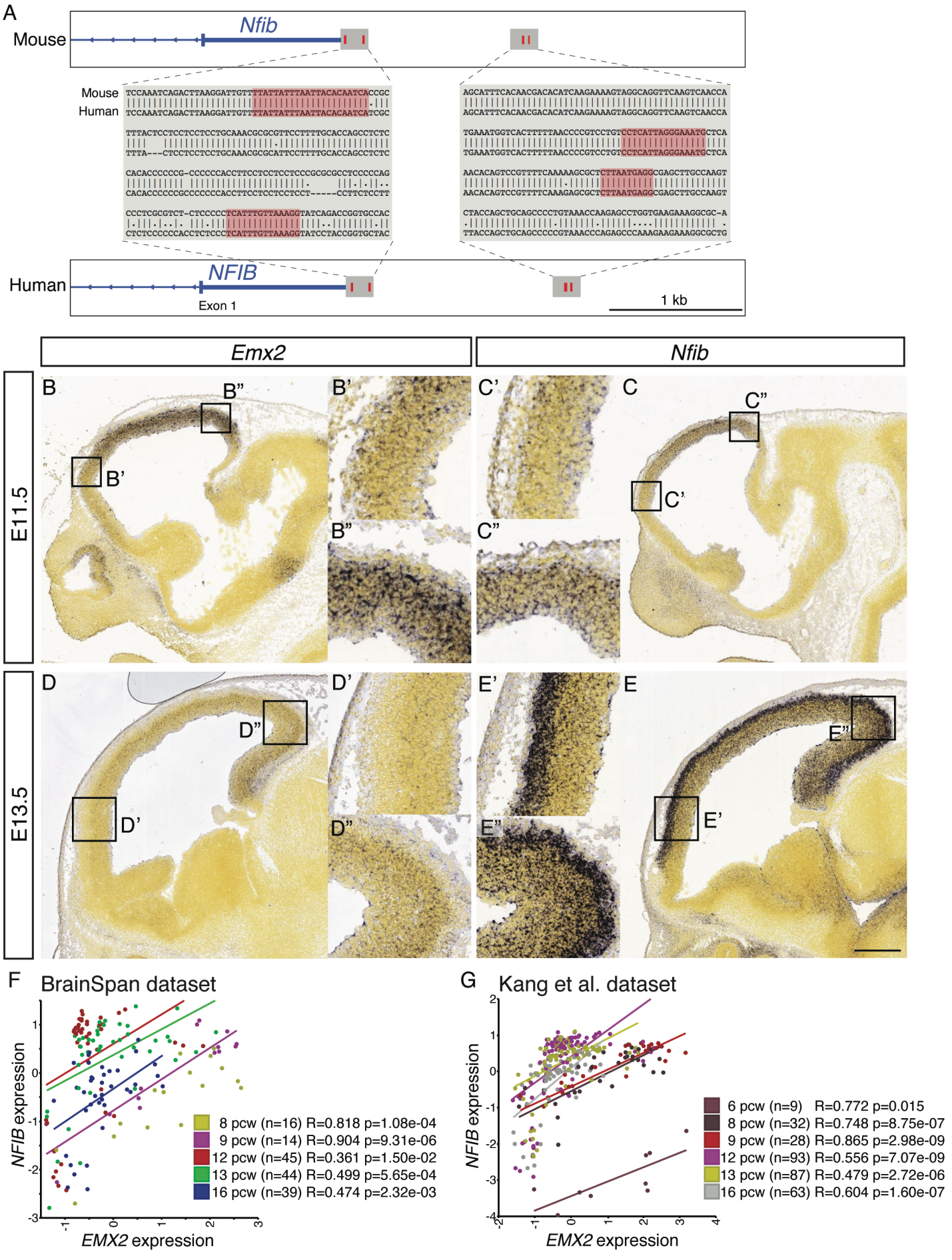
A
Mouse
Nfib
Mouse
Human
Human
NFIB
Exon 1
1 kb
Emx2
Nfib
E11.5
E13.5
B
B'
B"
C
C'
C"
D
D'
D"
E
E'
E"
F
BrainSpan dataset
NFIB expression
EMX2 expression
8 pcw (n=16) R=0.818 p=1.08e-04
9 pcw (n=14) R=0.904 p=9.31e-06
12 pcw (n=45) R=0.361 p=1.50e-02
13 pcw (n=44) R=0.499 p=5.65e-04
16 pcw (n=39) R=0.474 p=2.32e-03
G
Kang et al. dataset
NFIB expression
EMX2 expression
6 pcw (n=9) R=0.772 p=0.015
8 pcw (n=32) R=0.748 p=8.75e-07
9 pcw (n=28) R=0.865 p=2.98e-09
12 pcw (n=93) R=0.556 p=7.07e-09
13 pcw (n=87) R=0.479 p=2.72e-06
16 pcw (n=63) R=0.604 p=1.60e-07

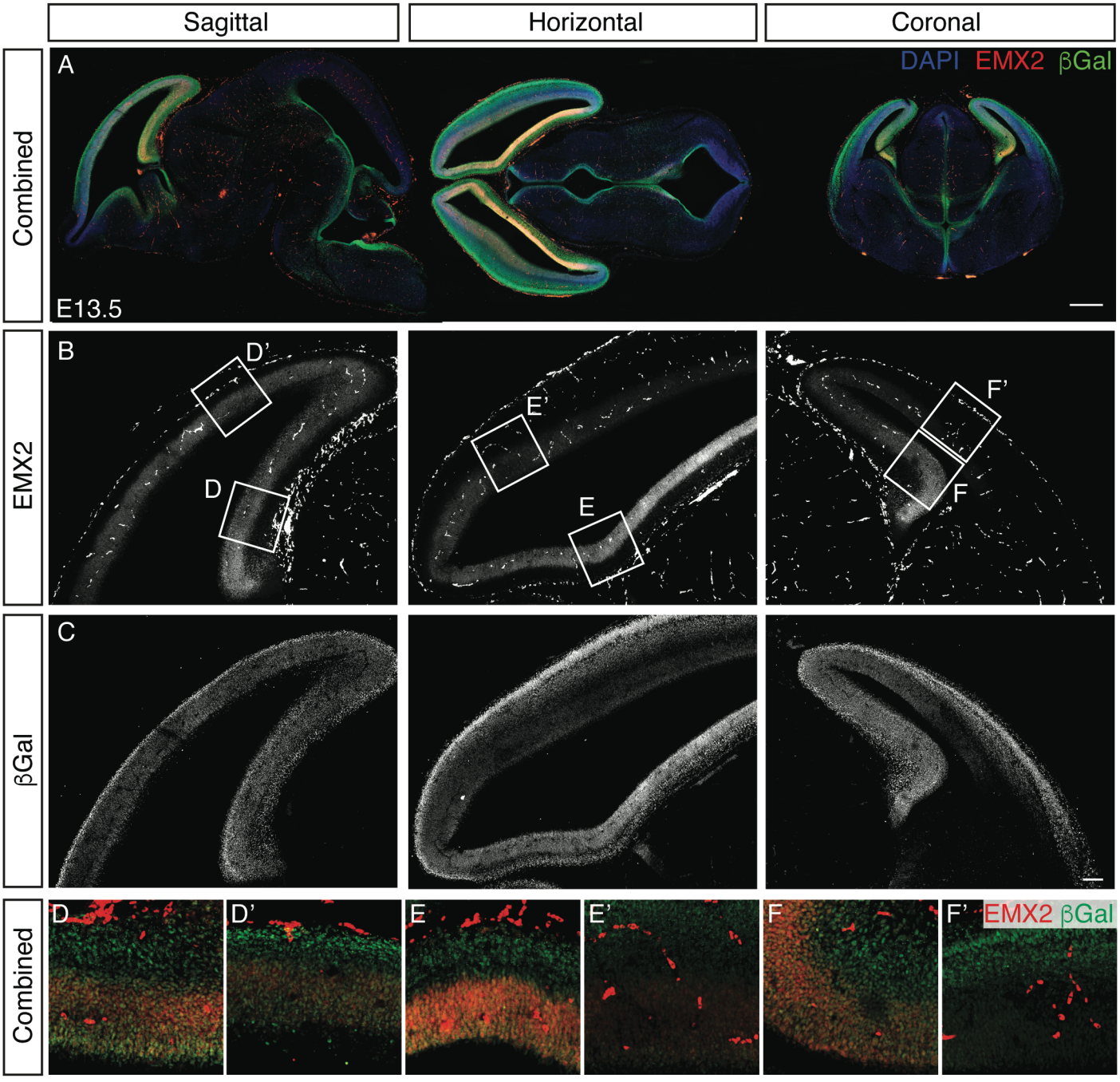
Sagittal
Horizontal
Coronal
Combined
A
DAPI EMX2 βGal
E13.5
EMX2
B
D'
D
E'
E
F'
F
βGal
C
Combined
D
D'
E
E'
F
F'
EMX2 βGal

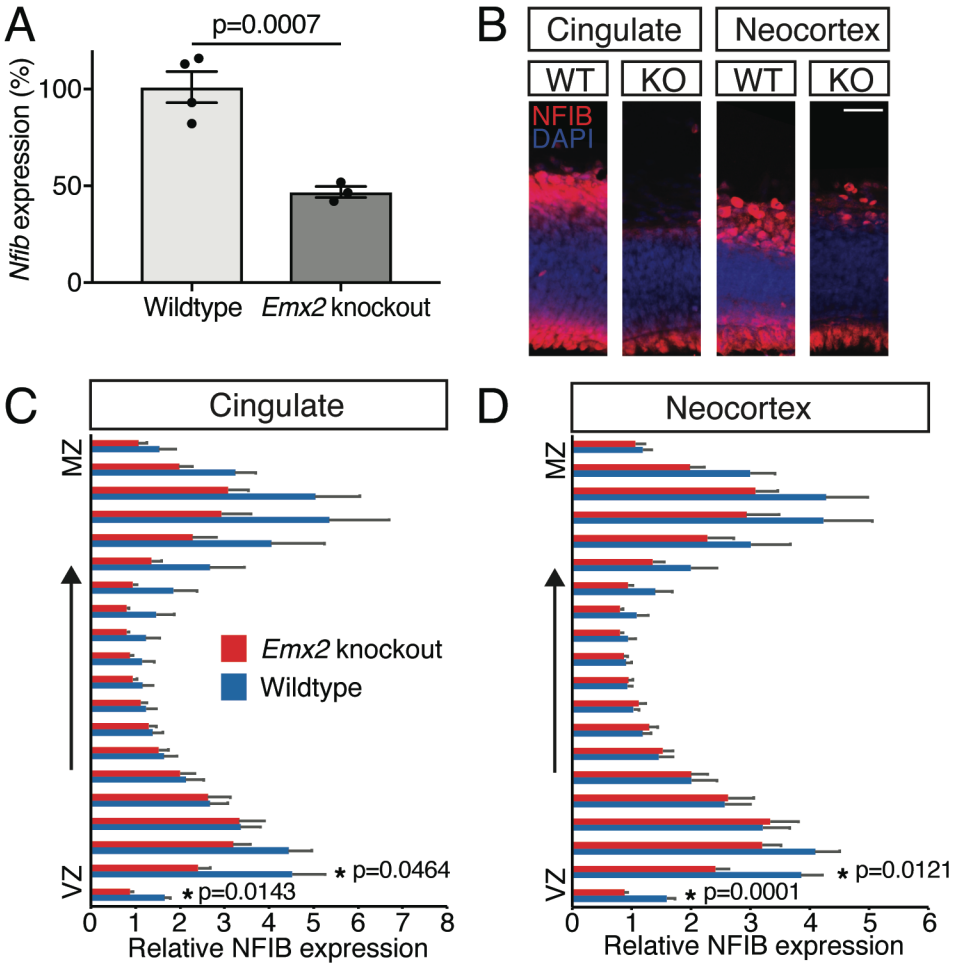
A
p=0.0007
Nfib expression (%)
100
50
0
Wildtype
Emx2 knockout
B
Cingulate
Neocortex
WT
KO
WT
KO
NFIB
DAPI
C
Cingulate
MZ
VZ
Emx2 knockout
Wildtype
* p=0.0464
* p=0.0143
0 1 2 3 4 5 6 7 8
Relative NFIB expression
D
Neocortex
MZ
VZ
* p=0.0121
* p=0.0001
0 1 2 3 4 5 6
Relative NFIB expression

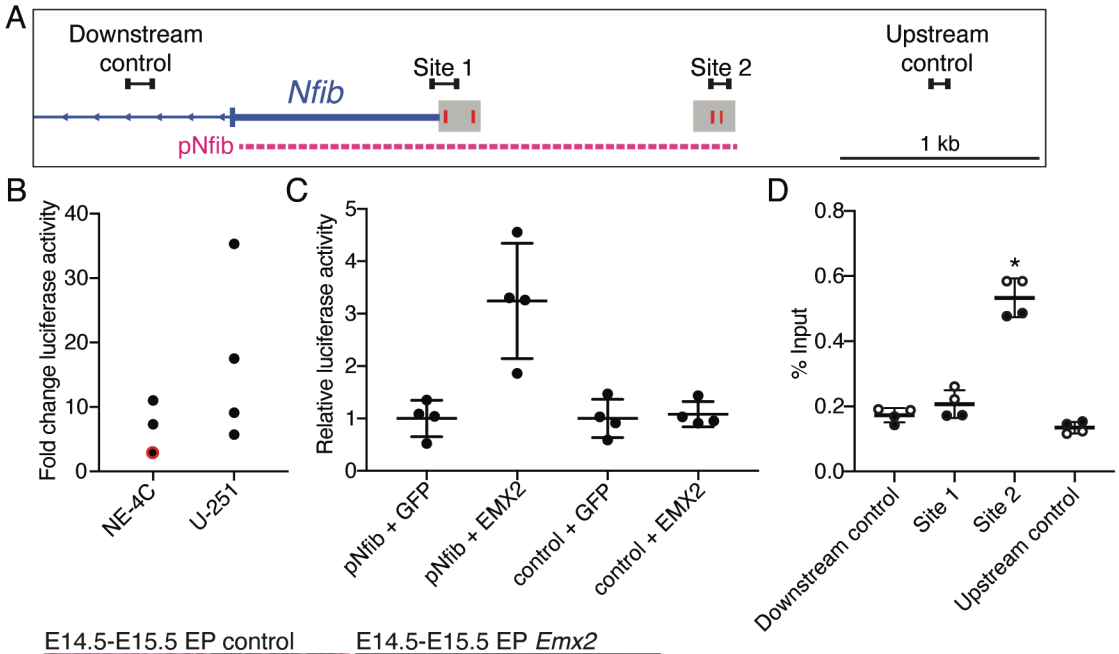
A
Downstream control
Site 1
Site 2
Upstream control
Nfib
pNfib
1 kb
B
Fold change luciferase activity
NE-4C
U-251
C
Relative luciferase activity
pNfib + GFP
pNfib + EMX2
control + GFP
control + EMX2
D
% Input
Downstream control
Site 1
Site 2
Upstream control

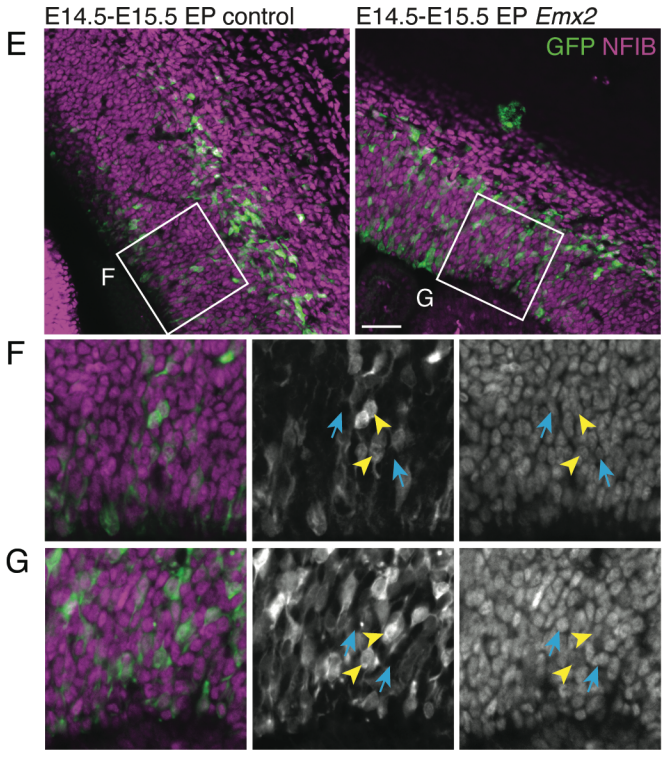
E14.5-E15.5 EP control
E14.5-E15.5 EP Emx2
GFP NFIB
E
F
G

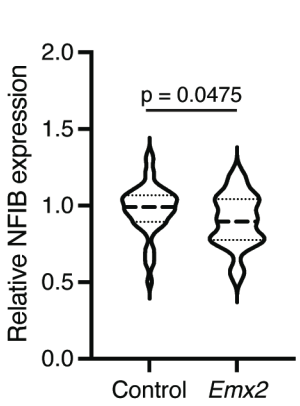
H
Relative NFIB expression
p = 0.0475
Control
Emx2